EC
Journals.ASM.org

A Visual Screen of Protein Localization during Sporulation Identifies New Components of Prospore Membrane-Associated Complexes in Budding Yeast

Chien Lam, Ethan Santore, Elizabeth Lavoie, Leor Needleman, Nicholas Fiacco, Carey Kim, Aaron M. Neiman

Department of Biochemistry and Cell Biology, Stony Brook University, Stony Brook, New York, USA

During ascospore formation in *Saccharomyces cerevisiae*, the secretory pathway is reorganized to create new intracellular compartments, termed prospore membranes. Prospore membranes engulf the nuclei produced by the meiotic divisions, giving rise to individual spores. The shape and growth of prospore membranes are constrained by cytoskeletal structures, such as septin proteins, that associate with the membranes. Green fluorescent protein (GFP) fusions to various proteins that associate with septins at the bud neck during vegetative growth as well as to proteins encoded by genes that are transcriptionally induced during sporulation were examined for their cellular localization during prospore membrane growth. We report localizations for over 100 different GFP fusions, including over 30 proteins localized to the prospore membrane compartment. In particular, the screen identified *IRC10* as a new component of the leading-edge protein complex (LEP), a ring structure localized to the lip of the prospore membrane. Localization of Irc10 to the leading edge is dependent on *SSP1*, but not *ADY3*. Loss of *IRC10* caused no obvious phenotype, but an *ady3 irc10* mutant was completely defective in sporulation and displayed prospore membrane morphologies similar to those of an *ssp1* strain. These results reveal the architecture of the LEP and provide insight into the evolution of this membrane-organizing complex.

Comprehensive localization studies have provided a wealth of information about the functions of different *Saccharomyces cerevisiae* proteins (1, 2). To date, most studies have examined protein localization only during mitotic growth in rich medium. The localization of proteins that are expressed only under specific conditions has not been systematically examined. Moreover, constitutively expressed proteins can also be relocalized under different conditions. Many examples of such changes in distribution occur when yeast cells undergo sporulation (3–6).

When diploid yeast cells are starved for nitrogen in the presence of a nonfermentable carbon source, they exit the mitotic cycle and enter the developmental program of meiosis and sporulation (7). Spores are created in an unusual cell division in which membranes are formed *de novo* in the cytosol and enclose each of the daughter nuclei produced by meiosis. These prospore membranes initially form on the cytoplasmic face of each of the four spindle pole bodies (SPBs) present in meiosis II. The membranes then expand beyond the SPBs to engulf the nuclei. As they do so, their shape is constrained by membrane-associated protein complexes.

One of these membrane-associated complexes, the leading-edge protein complex (LEP), composed of the proteins Ssp1, Ady3, and Don1, forms a ring structure at the lip of the prospore membrane (8–10). The LEP is organized in a stratified fashion, with *SSP1* being required for the localization of Ady3 and Don1 and *ADY3* being required for the localization of Don1. The LEP helps to control the shape of the prospore membrane and is proposed to exert an outward force that keeps the mouth of the prospore membrane open, in opposition to other proteins that promote membrane curvature and closure (11). Removal of the LEP at the end of meiosis II is essential for closure of the prospore membrane (12, 13).

In the course of meiosis and spore formation, several hundred genes are induced in coordinated waves of gene expression (14, 15). These induced genes can be further subdivided both by their time of expression (e.g., early genes and middle genes) and into those whose transcripts are detectable in vegetative cells but further induced during sporulation or those whose expression is detectable only in sporulating cells. While many of these sporulation-specific genes are required for progression through meiosis and spore morphogenesis, deletion studies have revealed clear phenotypes for only about 30% of these genes (16, 17). In addition to sporulation-specific genes, constitutively expressed proteins also play important roles in sporulation, and in some cases, these proteins are relocalized during sporulation (3–6).

The septin proteins, components of a second prospore membrane-associated complex, provide an example of the redistribution of vegetative functions during sporulation (3). In vegetative cells, septins localize to a ring at the bud neck. The septin ring has several important functions, including functions as a barrier to the diffusion of proteins between the mother and the bud, as a landmark to direct cytokinesis functions to the bud neck, and as a scaffold upon which different signal transduction pathways are organized (18–20). In contrast, in sporulating cells, septin rings at the plasma membrane disappear and the proteins localize as bars or sheets that extend along the nucleus-proximal bilayer of the prospore membrane from the leading edge toward the SPB (21). The organization of septins within these sheets is likely different

Received 16 December 2013 **Accepted** 27 December 2013

Published ahead of print 3 January 2014

Address correspondence to Aaron M. Neiman, aaron.neiman@stonybrook.edu.

Supplemental material for this article may be found at http://dx.doi.org/10.1128/EC.00333-13.

doi:10.1128/EC.00333-13

TABLE 1 Strains used in this study

Strain	Genotype	Reference or source
AN120	*MAT***a**/*MAT*α *ura3*/*ura3 leu2*/*leu2 trp1*::*hisG*/*trp1*::*hisG his3*Δ*SK*/*his3*Δ*SK lys2*/*lys2 arg4-Nsp1*/*ARG4 RME1*/*rme1*Δ::*LEU2 ho*Δ::*LYS2*/*ho*Δ::*LYS2*	5
AN246	AN120 plus *ady3*Δ::*kanMX6*/*ady3*Δ::*kanMX6*	10
CTL20	AN120 plus *irc10*Δ::*kanMX6*/*irc10*Δ::*kanMX6 ykr015c*Δ::*HIS3MX6*/*ykr015c*Δ::*HIS3MX6 yjl043w*::Δ*HphMX4*/*yjl043w*::Δ*HphMX4*	This study
CTL21	AN120 plus *ady3*Δ::*kanMX6*/*ady3*Δ::*kanMX6 irc10*Δ::*kanMX6*/*irc10*Δ::*kanMX6 ykr015c*Δ::*HIS3MX6*/*ykr015c*Δ::*HIS3MX6 yjl043w*::Δ*HphMX4*/*yjl043w*::Δ*HphMX4*	This study
CTL22	AN120 plus *ady3*Δ::*kanMX6*/*ady3*Δ::*kanMX6 ykr015c*Δ::*HIS3MX6*/*ykr015c*Δ::*HIS3MX6 yjl043w*::Δ*HphMX4*/*yjl043w*::Δ*HphMX4*	This study
CTL23	AN120 plus *ady3*Δ::*kanMX6*/*ady3*Δ::*kanMX6 irc10*Δ::*kanMX6*/*irc10*Δ::*kanMX6 ykr015c*Δ::*HIS3MX6*/*ykr015c*Δ::*HIS3MX6*	This study
CTL24	AN120 plus *ady3*Δ::*kanMX6*/*ady3*Δ::*kanMX6 irc10*Δ::*kanMX6*/*irc10*Δ::*kanMX6 yjl043w*::Δ*HphMX4*/*yjl043w*::Δ*HphMX4*	This study
CTL25	AN120 plus *ady3*Δ::*kanMX6*/*ady3*Δ::*kanMX6 irc10*Δ::*kanMX6*/*irc10*Δ::*kanMX6*	This study
CTL26	AN120 plus *don1*Δ::*HIS3MX6*/*don1*Δ::*HIS3MX6 irc10*Δ::*kanMX6*/*irc10*Δ::*kanMX6 ykr015c*Δ::*HIS3MX6*/*ykr015c*Δ::*HIS3MX6 yjl043w*::Δ*HphMX4*/*yjl043w*::Δ*HphMX4*	This study
NY551	AN120 plus *ssp1*Δ::*kanMX6*/*ssp1*Δ::*kanMX6*	This study
AN117-4B	*MAT*α *ura3 leu2 trp1*::*hisG his3*Δ*SK lys2 arg4-NspI rme1*Δ::*LEU2 ho*Δ::*LYS2*	5
CTL2	AN117-4B plus *irc10*Δ::*kanMX6 ykr015c*Δ::*HIS3MX6 yjl043w*::Δ*HphMX4*	This study
AN117-16D	*MAT***a** *ura3 leu2 trp1*::*hisG his3*Δ*SK lys2 ho*Δ::*LYS2*	5
MNH08	AN117-16D plus *don1*Δ::*HIS3MX6*	This study
AN1070	AN117-16D plus *ady3*Δ::*kanMX6*	10
GFP-tagged strains	*MAT***a** *ura3*Δ *leu2*Δ *his3*Δ *met15*Δ *GENEX*::*GFP*	2

from that in a septin ring both because of the different structure and because two of the vegetative septins, Cdc12 and Cdc11, are replaced with sporulation-specific paralogs, Spr3 and Spr28 (3, 22, 23). This change in composition raises the question of whether other proteins that colocalize with the septins at the bud neck still associate with septins at the prospore membrane.

To identify new proteins involved in prospore membrane assembly, the localization of green fluorescent protein (GFP) fusions to proteins encoded by over 300 sporulation-induced genes as well as 90 GFP fusions reported to localize to the bud neck in mitotic cells (2) was examined during meiosis II. Together, these two screens analyzed 435 GFP fusions, and we report the meiosis II localization of 113 fusion proteins. The results identify multiple new proteins localized to the prospore membrane, including new components of both the leading-edge complex and the septin complex. Characterization of the new leading-edge component, *IRC10*, provides insight into the evolution of this complex.

MATERIALS AND METHODS

Yeast media and strains. Standard yeast techniques and media were used (24). Strain genotypes are listed in Table 1. The GFP fusion strains used for screening were from the genome-wide GFP-tagged collection (2). To construct the triple mutant haploids, *IRC10* was deleted from strains AN117-4B and AN117-16D by PCR-mediated transformation using the *kanMX6* cassette (5, 25). *YKR015c* and *YJL043w* were then serially deleted from the AN117-4B *irc10*Δ strain using the *HIS3MX6* and *hphMX4* gene cassettes, respectively (25, 26). This MATα triple mutant haploid (CTL2) was mated to the *irc10*Δ mutant, sporulated, and dissected. CTL20 was constructed by mating of a *MAT***a** triple mutant segregant from that cross back to CTL2. To generate mutants in combination with *ady3*Δ, CTL2 was crossed to AN1070 (10), and the resulting diploid was sporulated and dissected. Because two *kanMX6* knockouts are segregating in this cross, all the mutants were confirmed by PCR analysis of the haploid segregants. Strains CTL21 to CTL25 were constructed by mating of segregants from that cross. Strain NY551 was made by PCR-mediated deletion of *SSP1* using *kanMX6* in strains AN117-4B and AN117-16D and was provided by H. Tachikawa. Strain CTL26 was constructed by mating of segregants from a cross of CTL2 to MNH08, a strain with a PCR-mediated knockout of *DON1* in strain AN117-16D provided by Mark Nickas.

GFP screen. For analysis, the *MAT***a** strains carrying the GFP fusions were pinned from 96-well plates to individual petri dishes in sets of 48. These patches were replica plated to synthetic-dextrose (SD) plates spread with a lawn of AN117-4B carrying pRS426-RFP-Spo20$^{51-91}$. Only diploids from mating between the strains can grow on this medium. After 2 days of incubation, patches were replica plated to a fresh SD plate, incubated overnight, and then replica plated to sporulation (SPO) medium. SPO plates were incubated from 16 to 20 h at room temperature before cells were transferred to microscope slides for examination. All diploids were analyzed on two separate days.

Plasmids. The high-copy-number plasmids carrying *YKR015c* and *YJL043w* are from the yeast tiling array collection (27). The prospore membrane marker pRS426-RFP-Spo20$^{51-91}$ and *DON1*::*GFP* plasmid pSB9 have been described elsewhere (21, 28). pRS426-IRC10::GFP was constructed by amplification of the *IRC10*::*GFP* fusion from the genome of the GFP tag collection haploid using the oligonucleotides CTO1 and MNO170, which engineered NotI and BglII restriction sites on either end of the fragment, respectively. After digestion with these two enzymes, the fragment was ligated into NotI-BamHI-digested pRS426 (29). pRS314-SSP1::YFP was constructed by digestion of pRS314-SSP1::HA (12) with AscI and PacI and replacement of the hemagglutinin (HA) tag with a yeast codon-optimized version of yellow fluorescent protein (YFP). This YFP gene was made by *de novo* synthesis (purchased from GeneWiz, NJ) and is flanked by AscI and PacI sites in pUC57. pRS314-SPR28-RFP was provided by H. Tachikawa. pRS426-PKC1-GFP was made by amplification of the *PKC1*::*GFP* fusion from chromosomal DNA using oligonucleotides BLO3 and HT66, which introduce XhoI and BglII sites at the 5′ and 3′ ends of the fragment, respectively. Following XhoI-BglII digestion, the PCR product was cloned into XhoI-BamHI-digested pRS426.

Electron microscopy. Cells were stained with $KMnO_4$ and prepared for electron microscopy as described previously (30). Images were collected on an FEI BioTwin12 microscope at 80 kV using an ATR digital camera.

TABLE 2 GFP fusion localizations

Protein and localization	Gene(s)
Proteins encoded by sporulation-induced genes	
Prospore membrane	
Peripheral	*YGR266w*, *CSR1*, *RRT5*, *YGL015c*, *MSO1*, *HUL4*, *VPS13*, *YNL018c*, *SSP2*, *SMA1*
Integral	*YFL040w*, *SMA2*, *YNL019c*
Secreted	*SGA1*, *SPR1*, *CDA1*, *YGL138c*
Punctate	*YCR030c*
Mitochondria	*FMP10*, *YIL055c*, *YLH47*, *SPR6*, *YGL230c*, *YKR005c*, *MRPS17*, *SRL4*
Nucleus	*RXT3*, *GIS1*, *VID22*, *GAT4*, *HTZ1*, *YDR018c*, *PTI1*, *DMC1*, *MND1*, *HOP1*, *SPO22*, *MEK1*, *MEI5*
Nuclear envelope/ER	*LAG1*, *POM34*, *CUE4*, *SPS22*,[a] *SPS2*,[a] *SCS2*, *GAS4*[a]
Lipid droplet	*NUS1*, *TGL4*, *TGL3*, *LDS1*, *SPS4*, *LDS2*, *SRT1*
Leading edge	*SSP1*, *IRC10*, *ADY3*
Spindle pole body	*CNM67*, *SPO74*, *SPO21*, *MPC54*, *SPC29*, *TUB4*
Spindle	*TUB3*
Cytoplasm	*PRD1*, *THR4*, *RVS167*, *YMR196w*, *PBP2*
Prospore cytoplasm	*YKL071w*, *FYV8*
Punctate cytoplasmic	*PEX22*, *SED4*, *YMR114c*, *MNE1*, *CHS5*, *YML119w*, *OSW2*, *DCI1*, *HRR25*, *YSP2*
Septin	*YSW1*, *SPR3*, *SPR28*
Vacuolar membrane	*YCK3*, *FET5*
Bud neck-localized proteins	
Prospore membrane (uniform)	*EXO84*, *SEC5*, *SEC3*, *YAP1802*, *SEC15*, *CHS7*, *SEC6*, *EXO70*, *APS2*, *BUD6*, *CBK1*, *BNI1*, *RGD1*, *BEM2*, *BUD2*, *KEL1*
Puncta on prospore membrane	*AKL1*, *SYP1*, *YAP1801*, *HOS3*, *SEC8*
Septins	*PKC1*, *CDC10*, *SHS1*, *CDC12*, *CDC11*
Prospore cytoplasm	*CMD1*
Mitochondria	*BEM1*

[a] The localization of Sps22, Sps2, and Gas4 to the endoplasmic reticulum is likely a fusion artifact (see the text).

Fluorescence microscopy. Images were collected on either a Zeiss Axioplan2 microscope with a Zeiss mRM digital camera or a Zeiss AxioObserver Z.1 microscope with a Hamamatsu ERG camera. Image stacks were deconvolved using Axiovision (version 4.7) software.

RESULTS

Localization of GFP fusion proteins during sporulation. To create the diploid cells necessary for sporulation studies, *MAT***a** strains from the genome-wide collection (2) carrying an integrated C-terminal GFP fusion under the control of the genes' native promoters were mated to a *MAT*α strain carrying the prospore membrane marker RFP-Spo20$^{51-91}$, consisting of red fluorescent protein (RFP) combined with Spo20 from residues 51 to 91 (28). The resulting diploids were sporulated on plates at 23°C for ~18 h and examined by fluorescence microscopy. Sporulating cells in the appropriate stage of meiosis were identified by the presence and morphology of the prospore membranes (12). Two factors were found to complicate the analysis of GFP localization. First, autofluorescence of the spore wall produced a signal at the spore periphery in the GFP channel in mature spores. Because of this autofluorescence, only cells displaying the small round or elongated prospore membrane morphology characteristic of cells in mid-meiosis II (12) were used to assess GFP localization. Second, due to the extensive autophagy occurring in sporulating cells, all the cells showed various degrees of GFP and RFP signals in the vacuolar lumen, presumably caused by incomplete degradation of the fusion proteins. This vacuolar signal particularly complicated the assessment of weak GFP signals. Therefore, localizations are reported only for those GFP fusions that were clearly distinguishable above the vacuolar background.

In all, 435 fusions were examined (for a complete list of fusions tested, see Table S1 in the supplemental material), and the various protein localization patterns seen for 113 fusions are listed in Table 2. The proteins were assigned to a variety of different locations, with the largest groups being the prospore membrane (31) and the nucleus (13). In addition, we identified a novel localization, as detailed below. Representative examples for different localization patterns are shown in Fig. 1.

Prospore membrane. From proteins encoded by sporulation-induced genes, 17 GFP fusions displayed uniform localization along the entire prospore membrane, as indicated by colocalization with the prospore membrane marker RFP-Spo20$^{51-91}$. On the basis of analysis of the predicted protein sequences, these fusions could be further divided into likely peripheral membrane proteins, integral membrane proteins, and secreted proteins whose fluorescence patterns represented localization to the lumen of the prospore membrane compartment. The predicted nature of each protein is listed in Table 2. The secreted proteins included Sga1, a glucoamylase capable of degrading both glycogen and starch (Fig. 1A to C) (32). On the basis of the biochemical fractionation of vegetative cells ectopically expressing Sga1, the protein had been reported to localize to the vacuole (32). Localization to the prospore membrane lumen suggests that the enzymatic activity of Sga1 is involved in spore wall assembly instead of storage carbohydrate metabolism.

The peripheral membrane proteins that localized to the prospore membrane included Vps13. Vps13 localizes to the endosome during vegetative growth (2). Thus, movement of Vps13 to the prospore membrane is an example of developmentally regulated relocalization (33). The importance of this movement is shown by the requirement for Vps13 from proper prospore membrane for-

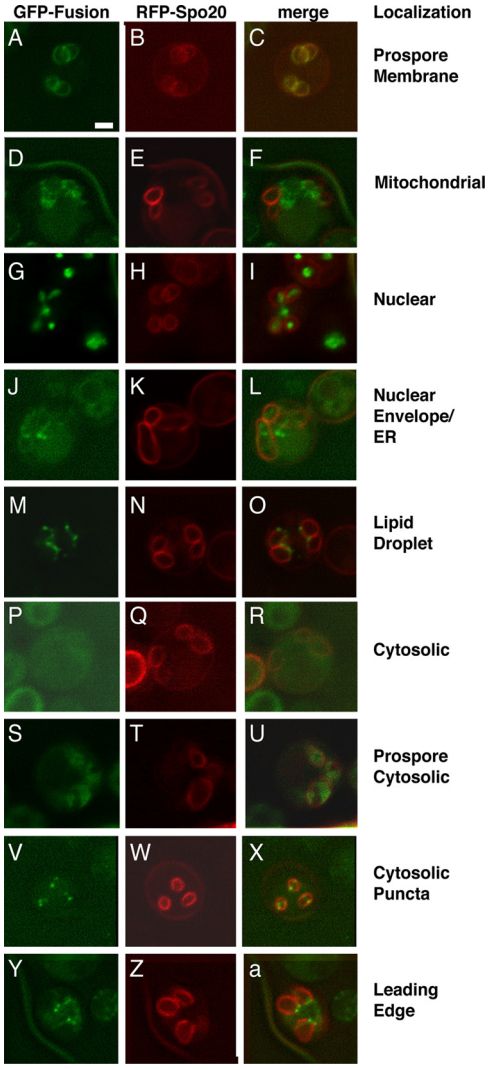

FIG 1 Different localization patterns for GFP fusions in meiosis II cells. Diploids expressing both a GFP fusion and the prospore membrane marker RFP-Spo20$^{51-91}$ were sporulated, and images of cells judged by prospore membrane morphology to be in meiosis II were collected. Representative examples for different localizations are shown. For each set of three images, the left panel shows the GFP fluorescence, the middle panel shows the prospore membrane, and right panel is the merged image. (A to C) Prospore membrane localization (Sga1-GFP); (D to F) mitochondrial localization (Mrps17-GFP); (G to I) nuclear localization (Htz1-GFP); (J to L) nuclear envelope/ER localization (Scs2-GFP); (M to O) lipid droplet localization (Tgl3-GFP); (P to R) cytosolic localization (Ymr196w-GFP); (S to U) prospore cytosol localization (Fyv8-GFP); (V to X) punctate localization (Sed4-GFP); (Y, Z, and a) leading-edge localization (Irc10-GFP). Images in panels A to C and G to I are projections through an image stack. Bar = 1 μm.

mation. Also notable among the peripheral membrane proteins was the presence of Ssp2 and Rrt5, which contain predicted RNA binding motifs. Earlier studies have suggested that some mRNAs are differentially localized between the ascal and spore cytoplasms (34). It is possible that localization of RNA binding proteins to the prospore membrane plays some role in this phenomenon.

Mitochondria. Eight sporulation-induced fusion proteins localized to mitochondria (Fig. 1D to F). Mitochondrial localization is indicated by concentration of the GFP signal in the region between the growing prospore membranes, with only limited entry of GFP inside the prospore membrane (28). Mitochondrial behavior is very different in sporulating and vegetative cells. The distribution of mitochondria within the cell is altered in sporulation, and the mechanisms by which they are segregated into daughter cells are different from those in mitotic growth (28, 35, 36). It is possible that these sporulation-specific mitochondrial proteins contribute to these changes in mitochondrial dynamics.

Nucleus. Localization to the nucleus is shown by concentration of the GFP signal into one round area within each of the developing spores. The complement of nucleus-localized proteins includes many for which this localization has previously been demonstrated (2, 31, 37–39). The nuclear proteins include a number of gene products involved in meiotic chromosome metabolism (Pch2, Dmc1, Mnd1, Hop1, Mek1, and Mei5), histones (Htz1) (Fig. 1G to I), and putative transcription factors (Gat4 and Gis1). Of note, the transcription factor Gis1 was localized to the nucleus throughout meiosis. *GIS1* is required for the induction of several genes late in the sporulation process, after meiosis is completed (16, 40). The continual localization of Gis1 to the nucleus indicates that its activity late in sporulation is not controlled by regulated nuclear import.

Several fusions displayed localization to the nuclear envelope/endoplasmic reticulum (ER) (Fig. 1J to L). This localization often appeared to be similar to the mitochondrial localization, with concentration in the area between the prospore membranes, but the GFP signal from the rims of the segregating nuclei within the prospore membrane could also be seen. In addition to proteins previously localized to this organelle (Scs2, Lag1, and Pom33), this set included three proteins (Sps2, Sps22, and Gas4) that are predicted to be glycosylphosphatidylinositol (GPI)-anchored spore wall components (16, 41). As carboxy-terminal GFP fusions were used in this study and the carboxyl-terminal transmembrane domain of GPI-anchored proteins is removed in the ER during attachment of the anchor (42), the GFP localization for these three proteins likely represents an artifact of the GFP fusion.

Lipid droplets. Seven fusions displayed a localization in which the proteins appeared to concentrate along one side of the prospore membrane (Fig. 1M to O). The GFP and RFP fluorescence often appeared to only partially overlap, suggesting that these proteins are adjacent to, rather than on, the membrane. Three of these gene products (Srt1, Tgl3, and Tgl4) have been reported to localize to lipid droplets in vegetative cells, and recently, it has been demonstrated that this pattern represents a subset of lipid droplets that associate specifically with the ascal side of prospore membranes (43). As lipid droplets do not associate with the plasma membrane in vegetative cells, this is a novel behavior for this organelle. The functional significance of the association between the lipid droplets and the prospore membrane remains to be determined.

Cytoplasm. Two different cytoplasmic localization patterns were identified in the screen. Some fusions, such as Ymr196w-GFP, were uniformly distributed throughout the cytoplasm, both inside and outside the prospore membranes (Fig. 1P to R). In contrast, the fusions to Fyv8 and Ykl071w concentrated within the presumptive spore cytoplasm inside the prospore membrane prior to membrane closure (Fig. 1S to U). Previously, we have seen that other GFP fusions can rapidly diffuse between the cytoplasms inside and outside the growing prospore membrane (12). Thus, concentration within the bounds of the prospore membrane suggests that some retention mechanism exists to concentrate Fyv8

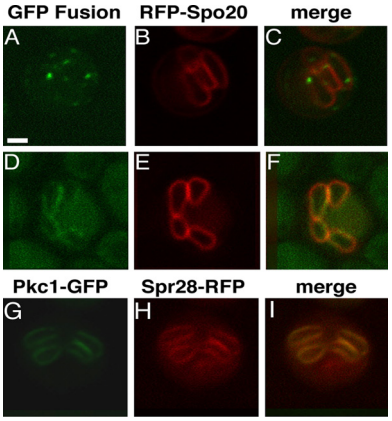

FIG 2 Localization patterns of bud neck proteins in meiosis II cells. For each set of three images, the left panel shows the GFP fluorescence, the middle panel shows the prospore membrane, and the right panel is the merged image. (A to C) Punctate pattern on the prospore membrane (Syp1-GFP) (A), prospore membranes of the cell in panel A (B), and merged image of panels A and B (C). (D to F) Septin localization (Pkc1-GFP) (D), prospore membranes of the cell in panel D (E), and merged image of panels D and E (F). (G to I) Pkc1 colocalizes with the septin Spr28. (G) Pkc1-GFP; (H) Spr28-RFP; (I) merged image of panels G and H. Bar = 1 μm.

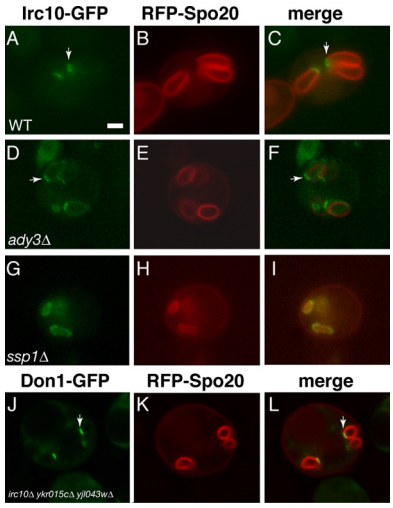

FIG 3 Localization of Irc10-GFP in LEP mutants. For each set of three images, the left panel shows the GFP fluorescence, the middle panel shows the prospore membrane, and right panel is the merged image. (A to C) Wild type (WT; AN120) expressing *IRC10*::*GFP* and RFP-Spo20$^{51-91}$; (D to F) an *ady3*Δ strain (AN246) expressing *IRC10*::*GFP* and RFP-Spo20$^{51-91}$; (G to I) an *ssp1*Δ strain (NY551) expressing *IRC10*::*GFP* and RFP-Spo20$^{51-91}$; (J to L) an *irc10*Δ *ykro15c*Δ *yjl043w*Δ strain (CTL20) expressing *DON1*::*GFP* and RFP-Spo20$^{51-91}$. Arrows, examples of GFP localization at the leading edge. Bar = 1 μm.

and Ykl071w within this region of the cytoplasm. This localization pattern has not been previously reported.

Cytoplasmic puncta. Several fusions displayed localization in multiple cytoplasmic puncta (e.g., Fig. 1V to X). In most cases, it is not clear what these puncta represent and whether the different puncta represent the same or different localizations for different proteins. On the basis of their reported localization in vegetative cells, it is likely that for Pex22 and Dci1 these puncta are peroxisomes, whereas for Hrr25 they may be *cis*-Golgi elements (44, 45).

Septin-associated proteins in sporulation. Among the proteins encoded by sporulation-induced genes analyzed, the only fusions found to localize to the septin complex were the previously known components Spr3, Spr28, and Ysw1 (3, 22, 46). The septin complex at the prospore membrane is arranged differently from that at the bud neck and appears as bars or sheets rather than as a ring (3, 21). To investigate whether proteins that colocalize with the septins at the bud neck would also associate with septins during sporulation, the localization of 90 GFP fusions reported to localize to the bud neck during vegetative growth was monitored in sporulating cells. Of these fusions, 28 produced clear localization patterns (Table 2; a complete list of fusions is provided in Table S1 in the supplemental material), a frequency comparable to that for the proteins encoded by sporulation-induced genes. There were three major classes of localization seen in these fusions. First, many of the GFP fusions displayed a uniform distribution around the prospore membrane. In particular, multiple subunits of the exocyst complex, which is known to be required for vesicle fusion at the prospore membrane, displayed this pattern (30). While these proteins clearly localized to the prospore membrane, they did not display any particular association with the septins, which were limited to a specific area of the prospore membrane. Second, several fusions localized at discrete foci along the prospore membrane (Fig. 2A to C). Third, five of the fusions displayed the bar-like pattern at the prospore membrane characteristic of septins. The last class included four known septins and the Pkc1 protein (Fig. 2D and E). To confirm this localization, the *PKC1*::*GFP* strain was crossed to a strain carrying an RFP fusion to the sporulation-specific septin SPR28, and colocalization of Pkc1 with Spr28 was examined. Pkc1-GFP clearly colocalized with septin bars in meiosis II cells (Fig. 2G to I). As septins at the prospore membrane can sometimes appear as patches, the fusions showing patchy localization were similarly examined for colocalization with Spr28-RFP. None of these fusions showed a consistent relationship to the position of the septins (unpublished observations). Thus, of all the bud neck-localized proteins examined, only one, Pkc1, displayed colocalization with the septins at the prospore membrane.

Characterization of a new LEP component. Our initial screen identified one new protein that localized to the leading edge of the prospore membrane, Irc10 (Fig. 1Y, Z, and a). The known components of the leading-edge complex are arranged in a stratified fashion with Ssp1, the key component that links the other proteins to the leading edge (9). To examine how Irc10 fits into this arrangement, Irc10-GFP localization was examined in *ssp1*Δ and *ady3*Δ strains. The *IRC10*::*GFP* fusion was first placed into a plasmid. When introduced into wild-type cells, Irc10-GFP expressed from the plasmid-borne allele produced a leading-edge localization similar to that of Irc10-GFP expressed from the integrated allele (Fig. 3A). In the *ady3*Δ strain, Irc10-GFP also showed distinct localization to the leading edge, though fainter localization around the prospore membrane was also visible. This indicates that the concentration of Irc10 at the leading edge is independent of *ADY3* (Fig. 3D). In contrast, in *ssp1*Δ cells, the Irc10-GFP signal was not seen at the leading edge but, rather, was distributed uniformly around the prospore membrane (Fig. 3G). Thus, Irc10 can localize to prospore membranes independently of other LEP components, but its concentration at the leading edge requires *SSP1*.

Sequence searches revealed two potential paralogs of *IRC10* in the *S. cerevisiae* genome, *YKR015c* and *YJL043w*. The region of the proteins with the highest homology to each other is an ~130-

FIG 4 A conserved Irc10 homology domain. Alignment of the N-terminal 130 amino acids of Irc10 with the two *S. cerevisiae* paralogs, Ykr015c and Yjl043w, as well as the orthologous proteins from three pre-whole-genome duplication species, *Zygosaccharomyces rouxii* (Z. roux), *Ashbya gossypii* (A. goss), and *Kluyveromyces lactis* (K. lac). In the consensus sequence, the letter f indicates a hydrophobic residue. Residues identical in at least 3 of the sequences are highlighted in bold.

amino-acid domain at the N termini. Iterative BLAST searches revealed that proteins with this domain are present in other yeast species as well, including *Ashbya gossypii* and *Kluyveromyces lactis* (Fig. 4), though only one family member is present in these other yeast genomes.

Interestingly, both *YKR015c* and *YJL043w* are also sporulation-induced genes (14, 15). We were, however, unable to detect any localization for the GFP fusions to *YKR015c* or *YJL043w* (unpublished observations). Strains with single gene deletions of *IRC10*, *YKR015c*, or *YJL043w* showed no sporulation defects (17). To test for possible redundancy, we constructed an *irc10*Δ *ykr015c*Δ *yjl043w*Δ triple mutant diploid and examined sporulation. No significant sporulation defect was seen in the triple mutant (Table 3). Consistent with the lack of phenotype, the localization of Don1-GFP to the leading edge was unaffected in the triple mutant (Fig. 3J). As *ADY3* is required for Don1 localization, this indicates that Ady3 is also at the leading edge in the *irc10*Δ *ykr015c*Δ *yjl043w*Δ mutant. Thus, Ady3/Don1 and Irc10 are independently recruited to the leading edge by Ssp1.

TABLE 3 Sporulation of LEP mutant strains

Genotype	% of strains with asci[a]	% of strains with the following no. of spores/ascus[b]:	
		1 or 2	3 or 4
WT	74	20	80
*irc10*Δ *ykr015c*Δ *yjl043w*Δ	76	36	64
*ady3*Δ	16	59	41
*ady3*Δ *irc10*Δ *ykr015c*Δ *yjl043w*Δ	<0.5		
*ady3*Δ *irc10*Δ *ykr015c*Δ	<0.5		
*ady3*Δ *irc10*Δ *yjl043w*Δ	<0.5		
*ady3*Δ *ykr015c*Δ *yjl043w*Δ	21	64	36
*ady3*Δ *irc10*Δ	<0.5		
*ady3*Δ *irc10*Δ/2μ-*YKR015c*	<0.5		
*ady3*Δ *irc10*Δ/2μ-*YJL043w*	<0.5		
*ady3*Δ *irc10*Δ/pRS314-*SSP1*::*YFP*	<0.5		
*ady3*Δ *irc10*Δ *ykr015c*Δ *yjl043w*Δ/p426-*IRC10*::*GFP*	8	85	15
*ssp1*Δ	<0.5		
*ssp1*Δ/pRS314-*SSP1*::*YFP*	17	72	28
*don1*Δ *irc10*Δ *ykr015c*Δ *yjl043w*Δ	79	35	65

[a] Percentages are the averages of three independent experiments. At least 200 cells were counted in each experiment.
[b] Percentages are the averages of three independent experiments. At least 200 asci were counted in each experiment.

***ADY3* and *IRC10* have overlapping functions.** The independent localization of Ady3 and Irc10 to prospore membranes raises the possibility that they play redundant roles at the leading edge. An *ady3*Δ strain was crossed to an *irc10*Δ *ykr015c*Δ *yjl043w*Δ triple mutant, and a quadruple mutant diploid, as well as various triple mutant combinations, was constructed. The quadruple mutant failed to sporulate, indicating that the combined loss of these leading-edge genes blocked spore formation (Table 3). Interestingly, an *ady3*Δ *ykr015c*Δ *yjl043w*Δ triple mutant sporulated well, whereas an *ady3*Δ *irc10*Δ double mutant failed to sporulate, suggesting that *IRC10* is specifically required in the absence of *ADY3* (Table 3). To assess whether *YKR015c* or *YJL043w* has any function at the leading edge, each gene was introduced into an *ady3*Δ *irc10*Δ strain on a high-copy-number plasmid. No rescue of the *ady3*Δ *irc10*Δ sporulation defect was seen with either gene, though the *IRC10*::*GFP* fusion largely rescued the sporulation defect (Table 3). Despite their homology to and coregulation with *IRC10*, it is unclear whether *YKR015c* or *YJL043w* plays any role during spore formation.

Deletion of *ADY3* removed both Ady3 and Don1 from the LEP. Therefore, the synthetic phenotype of *ady3*Δ and *irc10*Δ strains could conceivably be due to redundancy between *IRC10* and *DON1*. To test this, a *don1*Δ *irc10*Δ *ykr015c*Δ *yjl043w*Δ quadruple mutant was constructed and tested for sporulation (Table 3). This strain sporulated with an efficiency to similar that of both the *don1*Δ and *irc10*Δ *ykr015c*Δ *yjl043w*Δ strains, indicating that the loss of spore formation in the *ady3*Δ *irc10*Δ strain is due to functional overlap of *IRC10* with *ADY3* and not *DON1*.

An *ady3*Δ *irc10*Δ mutant phenocopies *ssp1*Δ. To determine the nature of the *ady3*Δ *irc10*Δ sporulation defect, cells were examined in a transmission electron microscope. In contrast to wild-type cells, where cytoplasmic material was found between the nuclear envelope and the prospore membrane (Fig. 5A and B), prospore membranes in *ady3*Δ *irc10*Δ cells were closely apposed to the nuclear envelope (Fig. 5C and D) and frequently appeared to close prematurely, resulting in the pinching off of fragments of the nucleus. These phenotypes are very reminiscent of those seen in *ssp1*Δ mutants, where there is no leading-edge complex (9) (Fig. 5E and F). In postmeiotic cells, prospore membranes in the *ady3*Δ

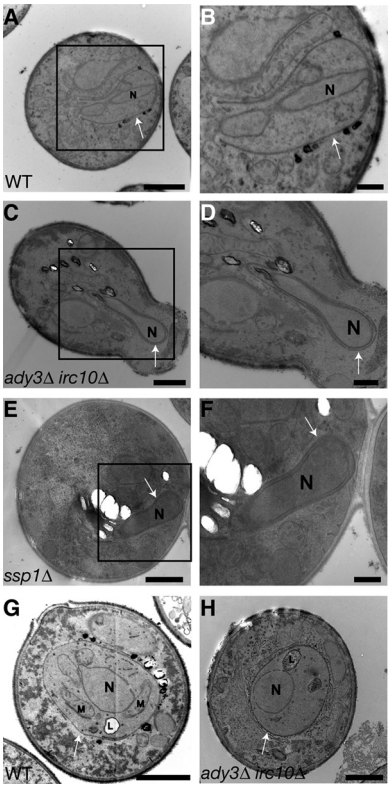

FIG 5 Prospore membrane morphology in *ady3*Δ *irc10*Δ cells. Strains were sporulated for 8 h before fixation and embedding for electron microscopy. (A) Prospore membrane in the wild type (AN120), indicated by an arrow. N, nucleus. (B) Higher magnification of the boxed area in panel A. (C) Prospore membrane in *ady3*Δ *irc10*Δ (CTL22), indicated by an arrow. (D) Higher magnification of the boxed area in panel C. (E) Prospore membrane in *ssp1*Δ (NY551), indicated by an arrow. (F) Higher magnification of the boxed area in panel E. (G) Prospore membrane, indicated by an arrow, in a postmeiotic WT cell. N, nucleus; M, mitochondrion; L, a lipid droplet. (H) Prospore membrane in a postmeiotic *ady3*Δ *irc10*Δ cell. Labels are as described for panel G. Bars = 1 μm (A, C, E, G, and H) and 500 nm (B, D, and F).

*irc10*Δ mutant rounded up and contained both nuclei and associated cytoplasm (Fig. 5H). However, no mitochondria were seen in the cytoplasm of these prospores, and spore development arrested at this stage.

The collapsed morphology of the prospore membrane during nuclear engulfment could be explained by loss of Ssp1 from the leading edge in the double mutant. To examine this possibility, a plasmid carrying an *SSP1*::*YFP* fusion was used to examine localization of Ssp1. The *SSP1*::*YFP* construct only partially complemented the sporulation defect of *ssp1*Δ cells (Table 3). Perhaps reflecting this partial function, when expressed in wild-type cells, the fusion localized to the leading edge but also to puncta along the prospore membrane (Fig. 6A to C). In the *ady3*Δ *irc10*Δ strain, fluorescence from Ssp1-YFP localized to the leading edge, and abnormal accumulation of fluorescence elsewhere on the prospore membrane was also seen (Fig. 6D to F). Though at least some Ssp1 was present at the leading edge, the prospore membrane morphology still appeared to be abnormal, and no sporulation was seen in the *ady3*Δ *irc10*Δ cells expressing *SSP1*::*YFP* (Table 3). *ADY3* and *IRC10* are, therefore, not required for Ssp1 to find the leading edge of the prospore membrane. However, in their absence, LEP function is compromised.

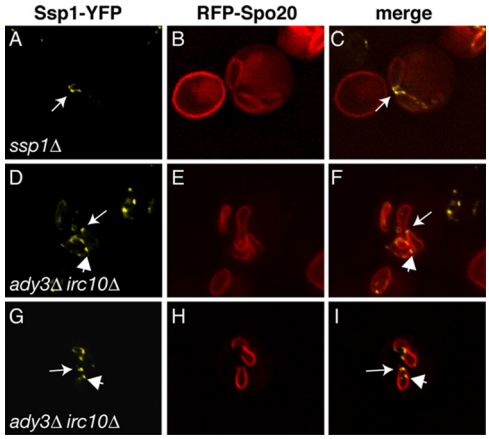

FIG 6 Localization of Ssp1 in *ady3*Δ *irc10*Δ cells. For each set of three images, the left panel shows the GFP fluorescence, the middle panel shows the prospore membrane, and the right panel is the merged image. (A to C) Wild type (AN120) expressing *SSP1*::*YFP* and RFP-Spo20$^{51\text{-}91}$; (D to F and G to I) an *ady3*Δ *irc10*Δ strain (CTL22) expressing *SSP1*::*YFP* and RFP-Spo20$^{51\text{-}91}$. Arrows, Ssp1-YFP puncta at the leading edge; arrowheads, puncta elsewhere on the prospore membrane. Bar = 1 μm.

DISCUSSION

Transcriptional studies have identified several hundred genes that are induced during sporulation. Though many of these genes are sporulation specific in their expression, only about 30% of the genes display a clear sporulation phenotype when deleted. In the absence of a mutant phenotype, the localization of the proteins may provide insight into their functions. Functional redundancy appears to be extensive between genes involved in sporulation (43). Generation of multiple mutant strains combining genes whose products have similar localizations, as shown here for *ADY3* and *IRC10*, might be an effective strategy to reveal functions for different gene products.

In vegetative cells, septin rings serve as scaffolds to localize many proteins important for cell signaling and cytokinesis and act as a barrier to diffusion between the mother and daughter cells. However, the role of septins in sporulation is unclear. Of 90 proteins reported to localize to the bud neck during vegetative growth, 28 displayed a clear localization in sporulating cells. Only one of these, Pkc1-GFP, colocalized with septins at the prospore membrane. The organization and composition of the septin filaments at the prospore membrane were distinct from those at the bud neck, and these results further distinguish the vegetative and sporulation septin complexes. The Glc7-Gip1 phosphatase colocalizes with the septins at the prospore membrane (21). These complexes thus contain both a phosphatase and a kinase. While the septins themselves are dispensable for sporulation, Gip1-Glc7 is necessary both for septin organization and for spore wall development (21, 22). The possible role of *PKC1* in spore formation remains to be explored.

Protein function in the leading-edge complex. The leading-edge complex is essential for proper spore formation. The ring at the prospore membrane lip acts to keep the mouth of the prospore membrane open during membrane expansion. In the *ady3*Δ *irc10*Δ mutant, Ssp1 could still localize to the leading edge. Nonetheless the membrane collapsed, as in an *ssp1*Δ strain. This indicates that either Ady3 or Irc10 is required for Ssp1 to form a stable

ring that can maintain the size of the prospore membrane opening. Thus, the minimal LEP consists of Ssp1 plus a stabilizing factor (Ady3 or Irc10). An *irc10*Δ mutant has no sporulation phenotype, while an *ady3*Δ mutant displays reduced spore formation due to a mitochondrial segregation defect (10), indicating that *ADY3* is somewhat more important for LEP function than *IRC10*. In light of the results described here, the mitochondrial segregation defect of *ady3*Δ may not reflect a direct role for *ADY3* in the transit of mitochondria into the spore. Rather, it may be that for a fraction of spores forming in *ady3*Δ cells, the prospore membrane opening is too small to accommodate the entry of mitochondria into the spores. The more extreme morphological defects seen in the *ady3*Δ *irc10*Δ cells may similarly explain the absence of mitochondria within postmeiotic prospore membranes in this mutant.

IRC10 was originally identified in a genome-wide screen for deletions that increase the frequency of Rad52 foci during vegetative growth, a phenotype suggestive of increased recombinational DNA repair in the mutant (47). No increased rate of recombination was seen in the *irc10*Δ mutant, however. Given the highly sporulation-induced expression of *IRC10* and its function at the leading edge described here, it is unclear how the mutant causes an alteration of Rad52 localization, though at least one other highly sporulation-induced gene, *IRC18*/*OSW6*, was identified in the same screen (14, 47).

Evolution of the LEP. Ascospore formation is cytologically similar in all yeasts and requires analogous protein complexes. However, where the proteins of these complexes have been identified, there is often no homology between proteins of orthologous structures in different yeasts. For example, in both *S. pombe* and *S. cerevisiae*, a vesicle-docking complex on the cytoplasmic surface of the spindle pole body serves as the initiation site for prospore membrane assembly, yet the protein components of these structures are unrelated (48). Similarly, the *S. pombe* analog of Ssp1, the leading-edge protein Meu14, is not related by sequence to the *S. cerevisiae* protein (49). The discovery of functional overlap between Ady3 and Irc10 provides insight into how changes in the protein components can occur within essential complexes.

Proteins related to Ssp1 and Irc10 can be found in species such as *A. gossypii* and *K. lactis* that diverged from *S. cerevisiae* prior to the whole-genome duplication event (50, 51). The transcription of the *A. gossypii* ortholog of *IRC10*, *AFR221w*, was recently reported to be increased in sporulating cells, suggesting that it may similarly function in sporulation (52). In contrast, *ADY3* arose from the whole-genome duplication as a second copy of the *CNM67* gene, encoding a constitutive SPB component (50, 51, 53). Therefore, there is no direct *ADY3* ortholog present in *A. gossypii* or *K. lactis*.

Ssp1 transiently interacts with SPB components early in prospore membrane formation (9). One possible scenario for the evolution of *ADY3*, therefore, is that the duplication of *CNM67* allowed one copy (*ADY3*) to diverge and maintain an interaction with Ssp1 at the leading edge, and maintenance of the Ady3-SspI interaction relieved the need for Irc10 at the leading edge. Why, then, does *S. cerevisiae* retain *IRC10*? One possibility is that *IRC10* is still required for sporulation under conditions different from those used in the laboratory. Alternatively, as *ADY3* is more important for leading-edge function than *IRC10* in *S. cerevisiae*, it may be that *S. cerevisiae* is an example of an organism in the process of replacing a component of a complex essential for sporulation with an unrelated protein. Testing this hypothesis will require examining the phenotypes and localization of *SSP1*, *IRC10*, and *CNM67* orthologs in yeast such as *A. gossypii*.

In sum, we conducted a systematic visual screen of the localization of proteins during sporulation. The results of this screen provide insight into a variety of processes and complexes, including sporulation-specific organellar proteins, new components of known protein complexes, and a novel localization pattern requiring further investigation. Though only about 7% of the GFP fusion collection was examined in the screen, the methodology described could be adapted to automated platforms to allow screening of the entire collection.

ACKNOWLEDGMENTS

We are indebted to Maya Schuldiner (Weizman Institute) for the GFP fusion strains, to Hiroyuki Tachikawa (University of Tokyo) for strains and plasmids, and to Mark Nickas for strains. Nancy Hollingsworth and Jae-Sook Park provided helpful comments on the manuscript. We are grateful to Susan Van Horn in the Stony Brook Central Microscopy Imaging Center for assistance with electron microscopy.

This work was supported by NIH grant GM072540 to A.M.N. E.S. and N.F. were supported by Simons Summer Research Fellowships.

REFERENCES

1. **Breker M, Gymrek M, Schuldiner M.** 2013. A novel single-cell screening platform reveals proteome plasticity during yeast stress responses. J. Cell Biol. **200:**839–850. http://dx.doi.org/10.1083/jcb.201301120.
2. **Huh WK, Falvo JV, Gerke LC, Carroll AS, Howson RW, Weissman JS, O'Shea EK.** 2003. Global analysis of protein localization in budding yeast. Nature **425:**686–691. http://dx.doi.org/10.1038/nature02026.
3. **Fares H, Goetsch L, Pringle JR.** 1996. Identification of a developmentally regulated septin and involvement of the septins in spore formation in *Saccharomyces cerevisiae*. J. Cell Biol. **132:**399–411. http://dx.doi.org/10.1083/jcb.132.3.399.
4. **Morishita M, Mendonsa R, Wright J, Engebrecht J.** 2007. Snc1p v-SNARE transport to the prospore membrane during yeast sporulation is dependent on endosomal retrieval pathways. Traffic **8:**1231–1245. http://dx.doi.org/10.1111/j.1600-0854.2007.00606.x.
5. **Neiman AM, Katz L, Brennwald PJ.** 2000. Identification of domains required for developmentally regulated SNARE function in *Saccharomyces cerevisiae*. Genetics **155:**1643–1655.
6. **Rudge SA, Morris AJ, Engebrecht J.** 1998. Relocalization of phospholipase D activity mediates membrane formation during meiosis. J. Cell Biol. **140:**81–90. http://dx.doi.org/10.1083/jcb.140.1.81.
7. **Neiman AM.** 2011. Sporulation in the budding yeast *Saccharomyces cerevisiae*. Genetics **189:**737–765. http://dx.doi.org/10.1534/genetics.111.127126.
8. **Knop M, Strasser K.** 2000. Role of the spindle pole body of yeast in mediating assembly of the prospore membrane during meiosis. EMBO J. **19:**3657–3667. http://dx.doi.org/10.1093/emboj/19.14.3657.
9. **Moreno-Borchart AC, Strasser K, Finkbeiner MG, Shevchenko A, Shevchenko A, Knop M.** 2001. Prospore membrane formation linked to the leading edge protein (LEP) coat assembly. EMBO J. **20:**6946–6957. http://dx.doi.org/10.1093/emboj/20.24.6946.
10. **Nickas ME, Neiman AM.** 2002. Ady3p links spindle pole body function to spore wall synthesis in *Saccharomyces cerevisiae*. Genetics **160:**1439–1450.
11. **Maier P, Rathfelder N, Maeder CI, Colombelli J, Stelzer EH, Knop M.** 2008. The SpoMBe pathway drives membrane bending necessary for cytokinesis and spore formation in yeast meiosis. EMBO J. **27:**2363–2374. http://dx.doi.org/10.1038/emboj.2008.168.
12. **Diamond A, Park JS, Inoue I, Tachikawa H, Neiman AM.** 2008. The anaphase promoting complex targeting subunit Ama1 links meiotic exit to cytokinesis during sporulation in *Saccharomyces cerevisiae*. Mol. Biol. Cell **20:**134–145. http://dx.doi.org/10.1091/mbc.E08-06-0615.
13. **Maier P, Rathfelder N, Finkbeiner MG, Taxis C, Mazza M, Le Panse S, Haguenauer-Tsapis R, Knop M.** 2007. Cytokinesis in yeast meiosis depends on the regulated removal of Ssp1p from the prospore membrane. EMBO J. **26:**1843–1852. http://dx.doi.org/10.1038/sj.emboj.7601621.
14. **Chu S, DeRisi J, Eisen M, Mulholland J, Botstein D, Brown PO, Herskowitz I.** 1998. The transcriptional program of sporulation in bud-

ding yeast. Science **282:**699–705. http://dx.doi.org/10.1126/science.282.5389.699.
15. **Primig M, Williams RM, Winzeler EA, Tevzadze GG, Conway AR, Hwang SY, Davis RW, Esposito RE.** 2000. The core meiotic transcriptome in budding yeasts. Nat. Genet. **26:**415–423. http://dx.doi.org/10.1038/82539.
16. **Coluccio A, Bogengruber E, Conrad MN, Dresser ME, Briza P, Neiman AM.** 2004. Morphogenetic pathway of spore wall assembly in *Saccharomyces cerevisiae*. Eukaryot. Cell **3:**1464–1475. http://dx.doi.org/10.1128/EC.3.6.1464-1475.2004.
17. **Rabitsch KP, Toth A, Galova M, Schleiffer A, Schaffner G, Aigner E, Rupp C, Penkner AM, Moreno-Borchart AC, Primig M, Esposito RE, Klein F, Knop M, Nasmyth K.** 2001. A screen for genes required for meiosis and spore formation based on whole-genome expression. Curr. Biol. **11:**1001–1009. http://dx.doi.org/10.1016/S0960-9822(01)00274-3.
18. **DeMarini DJ, Adams AE, Fares H, De Virgilio C, Valle G, Chuang JS, Pringle JR.** 1997. A septin-based hierarchy of proteins required for localized deposition of chitin in the *Saccharomyces cerevisiae* cell wall. J. Cell Biol. **139:**75–93. http://dx.doi.org/10.1083/jcb.139.1.75.
19. **Barral Y, Mermall V, Mooseker MS, Snyder M.** 2000. Compartmentalization of the cell cortex by septins is required for maintenance of cell polarity in yeast. Mol. Cell **5:**841–851. http://dx.doi.org/10.1016/S1097-2765(00)80324-X.
20. **Lippincott J, Li R.** 1998. Sequential assembly of myosin II, an IQGAP-like protein, and filamentous actin to a ring structure involved in budding yeast cytokinesis. J. Cell Biol. **140:**355–366. http://dx.doi.org/10.1083/jcb.140.2.355.
21. **Tachikawa H, Bloecher A, Tatchell K, Neiman AM.** 2001. A Gip1p-Glc7p phosphatase complex regulates septin organization and spore wall formation. J. Cell Biol. **155:**797–808. http://dx.doi.org/10.1083/jcb.200107008.
22. **De Virgilio C, DeMarini DJ, Pringle JR.** 1996. *SPR28*, a sixth member of the septin gene family in *Saccharomyces cerevisiae* that is expressed specifically in sporulating cells. Microbiology **142:**2897–2905. http://dx.doi.org/10.1099/13500872-142-10-2897.
23. **McMurray MA, Thorner J.** 2008. Septin stability and recycling during dynamic structural transitions in cell division and development. Curr. Biol. **18:**1203–1208. http://dx.doi.org/10.1016/j.cub.2008.07.020.
24. **Rose MD, Fink GR.** 1990. Methods in yeast genetics. Cold Spring Harbor Laboratory Press, Cold Spring Harbor, NY.
25. **Longtine MS, McKenzie A, III, Demarini DJ, Shah NG, Wach A, Brachat A, Philippsen P, Pringle JR.** 1998. Additional modules for versatile and economical PCR-based gene deletion and modification in *Saccharomyces cerevisiae*. Yeast **14:**953–961.
26. **Janke C, Magiera MM, Rathfelder N, Taxis C, Reber S, Maekawa H, Moreno-Borchart A, Doenges G, Schwob E, Schiebel E, Knop M.** 2004. A versatile toolbox for PCR-based tagging of yeast genes: new fluorescent proteins, more markers and promoter substitution cassettes. Yeast **21:**947–962. http://dx.doi.org/10.1002/yea.1142.
27. **Jones GM, Stalker J, Humphray S, West A, Cox T, Rogers J, Dunham I, Prelich G.** 2008. A systematic library for comprehensive overexpression screens in *Saccharomyces cerevisiae*. Nat. Methods **5:**239–241. http://dx.doi.org/10.1038/nmeth.1181.
28. **Suda Y, Nakanishi H, Mathieson EM, Neiman AM.** 2007. Alternative modes of organellar segregation during sporulation in *Saccharomyces cerevisiae*. Eukaryot. Cell **6:**2009–2017. http://dx.doi.org/10.1128/EC.00238-07.
29. **Sikorski RS, Hieter P.** 1989. A system of shuttle vectors and yeast host strains designed for efficient manipulation of DNA in *Saccharomyces cerevisiae*. Genetics **122:**19–27.
30. **Neiman AM.** 1998. Prospore membrane formation defines a developmentally regulated branch of the secretory pathway in yeast. J. Cell Biol. **140:**29–37. http://dx.doi.org/10.1083/jcb.140.1.29.
31. **San-Segundo PA, Roeder GS.** 1999. Pch2 links chromatin silencing to meiotic checkpoint control. Cell **97:**313–324. http://dx.doi.org/10.1016/S0092-8674(00)80741-2.
32. **Pugh TA, Shah JC, Magee PT, Clancy MJ.** 1989. Characterization and localization of the sporulation glucoamylase of *Saccharomyces cerevisiae*. Biochim. Biophys. Acta **994:**200–209. http://dx.doi.org/10.1016/0167-4838(89)90294-X.
33. **Park JS, Neiman AM.** 2012. *VPS13* regulates membrane morphogenesis during sporulation in *Saccharomyces cerevisiae*. J. Cell Sci. **125**(Pt 12)**:**3004–3011. http://dx.doi.org/10.1242/jcs.105114.
34. **Kurtz S, Lindquist S.** 1986. Subcellular differentiation in sporulating yeast cells. Cell **45:**771–779. http://dx.doi.org/10.1016/0092-8674(86)90791-9.
35. **Gorsich SW, Shaw JM.** 2004. Importance of mitochondrial dynamics during meiosis and sporulation. Mol. Biol. Cell **15:**4369–4381. http://dx.doi.org/10.1091/mbc.E03-12-0875.
36. **Miyakawa I, Aoi H, Sando N, Kuroiwa T.** 1984. Fluorescence microscopic studies of mitochondrial nucleoids during meiosis and sporulation in the yeast, *Saccharomyces cerevisiae*. J. Cell Sci. **66:**21–38.
37. **Bishop DK.** 1994. RecA homologs Dmc1 and Rad51 interact to form multiple nuclear complexes prior to meiotic chromosome synapsis. Cell **79:**1081–1092. http://dx.doi.org/10.1016/0092-8674(94)90038-8.
38. **Burns N, Grimwade B, Ross-Macdonald PB, Choi EY, Finberg K, Roeder GS, Snyder M.** 1994. Large-scale analysis of gene expression, protein localization, and gene disruption in *Saccharomyces cerevisiae*. Genes Dev. **8:**1087–1105. http://dx.doi.org/10.1101/gad.8.9.1087.
39. **Hollingsworth NM, Goetsch L, Byers B.** 1990. The *HOP1* gene encodes a meiosis-specific component of yeast chromosomes. Cell **61:**73–84. http://dx.doi.org/10.1016/0092-8674(90)90216-2.
40. **Yu Y, Neiman AM, Sternglanz R.** 2010. The JmjC domain of Gis1 is dispensable for transcriptional activation. FEMS Yeast Res. **10:**793–801. http://dx.doi.org/10.1111/j.1567-1364.2010.00680.x.
41. **Caro LH, Tettelin H, Vossen JH, Ram AF, van den Ende H, Klis FM.** 1997. In silicio identification of glycosyl-phosphatidylinositol-anchored plasmamembrane and cell wall proteins of *Saccharomyces cerevisiae*. Yeast **13:**1477–1489. http://dx.doi.org/10.1002/(SICI)1097-0061(199712)13:15<1477::AID-YEA184>3.0.CO;2-L.
42. **Orlean P.** 2012. Architecture and biosynthesis of the *Saccharomyces cerevisiae* cell wall. Genetics **192:**775–818. http://dx.doi.org/10.1534/genetics.112.144485.
43. **Lin CP, Kim C, Smith SO, Neiman AM.** 2013. A highly redundant gene network controls assembly of the outer spore wall in *S. cerevisiae*. PLoS Genet. **9:**e1003700. http://dx.doi.org/10.1371/journal.pgen.1003700.
44. **Geisbrecht BV, Schulz K, Nau K, Geraghty MT, Schulz H, Erdmann R, Gould SJ.** 1999. Preliminary characterization of Yor180Cp: identification of a novel peroxisomal protein of *Saccharomyces cerevisiae* involved in fatty acid metabolism. Biochem. Biophys. Res. Commun. **260:**28–34. http://dx.doi.org/10.1006/bbrc.1999.0860.
45. **Lord C, Bhandari D, Menon S, Ghassemian M, Nycz D, Hay J, Ghosh P, Ferro-Novick S.** 2011. Sequential interactions with Sec23 control the direction of vesicle traffic. Nature **473:**181–186. http://dx.doi.org/10.1038/nature09969.
46. **Ishihara M, Suda Y, Inoue I, Tanaka T, Takahashi T, Gao XD, Fukui Y, Ihara S, Neiman AM, Tachikawa H.** 2009. Protein phosphatase type 1-interacting protein Ysw1 is involved in proper septin organization and prospore membrane formation during sporulation. Eukaryot. Cell **8:**1027–1037. http://dx.doi.org/10.1128/EC.00095-09.
47. **Alvaro D, Lisby M, Rothstein R.** 2007. Genome-wide analysis of Rad52 foci reveals diverse mechanisms impacting recombination. PLoS Genet. **3:**e228. http://dx.doi.org/10.1371/journal.pgen.0030228.
48. **Shimoda C.** 2004. Forespore membrane assembly in yeast: coordinating SPBs and membrane trafficking. J. Cell Sci. **117:**389–396. http://dx.doi.org/10.1242/jcs.00980.
49. **Okuzaki D, Satake W, Hirata A, Nojima H.** 2003. Fission yeast *meu14+* is required for proper nuclear division and accurate forespore membrane formation during meiosis II. J. Cell Sci. **116:**2721–2735. http://dx.doi.org/10.1242/jcs.00496.
50. **Byrne KP, Wolfe KH.** 2005. The Yeast Gene Order Browser: combining curated homology and syntenic context reveals gene fate in polyploid species. Genome Res. **15:**1456–1461. http://dx.doi.org/10.1101/gr.3672305.
51. **Wolfe KH, Shields DC.** 1997. Molecular evidence for an ancient duplication of the entire yeast genome. Nature **387:**708–713. http://dx.doi.org/10.1038/42711.
52. **Wasserstrom L, Lengeler KB, Walther A, Wendland J.** 2013. Molecular determinants of sporulation in *Ashbya gossypii*. Genetics **195:**87–99. http://dx.doi.org/10.1534/genetics.113.151019.
53. **Schaerer F, Morgan G, Winey M, Philippsen P.** 2001. Cnm67p is a spacer protein of the *Saccharomyces cerevisiae* spindle pole body outer plaque. Mol. Biol. Cell **12:**2519–2533. http://dx.doi.org/10.1091/mbc.12.8.2519.